

Solution Nuclear Magnetic Resonance Structure and Molecular Dynamics Simulations of a Murine 18.5 kDa Myelin Basic Protein Segment (S72–S107) in Association with Dodecylphosphocholine Micelles

Mumdooh A. M. Ahmed,^{†,‡,§} Miguel De Avila,[†] Eugenia Polverini,^{||} Kyrylo Bessonov,[†] Vladimir V. Bamm,[†] and George Harauz^{*,†}

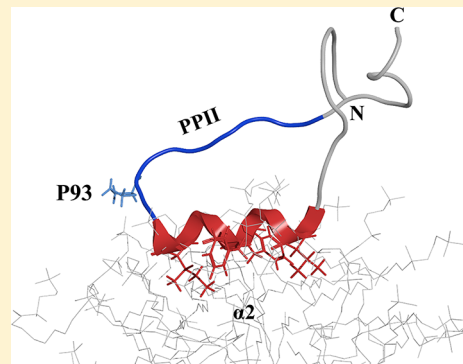
[†]Department of Molecular and Cellular Biology and [‡]Department of Physics, University of Guelph, 50 Stone Road East, Guelph, Ontario N1G 2W1, Canada

[§]Department of Physics, Faculty of Science at Suez, Suez-Canal University, Suez, Egypt

^{||}Department of Physics, University of Parma, V. le Usberti, 7/A-Campus, 43124 Parma, Italy

Supporting Information

ABSTRACT: The 18.5 kDa myelin basic protein (MBP), the most abundant splice isoform in adult mammalian myelin, is a multifunctional, intrinsically disordered protein involved in the development and compaction of the myelin sheath in the central nervous system. A highly conserved central segment comprises a membrane-anchoring amphipathic α -helix followed by a proline-rich segment that represents a ligand for SH3 domain-containing proteins. Here, we have determined using solution nuclear magnetic resonance spectroscopy the structure of a 36-residue peptide fragment of MBP (murine 18.5 kDa residues S72–S107, denoted the α 2-peptide) comprising these two structural motifs, in association with dodecylphosphocholine (DPC) micelles. The structure was calculated using CS-ROSETTA (version 1.01) because the nuclear Overhauser effect restraints were insufficient for this protein. The experimental studies were complemented by molecular dynamics simulations of a corresponding 24-residue peptide fragment (murine 18.5 kDa residues E80–G103, denoted the MD-peptide), also in association with a DPC micelle *in silico*. The experimental and theoretical results agreed well with one another, despite the independence of the starting structures and analyses, both showing membrane association via the amphipathic α -helix, and a sharp bend in the vicinity of the Pro93 residue (murine 18.5 kDa sequence numbering). Overall, the conformations elucidated here show how the SH3 ligand is presented to the cytoplasm for interaction with SH3 domain-containing proteins such as Fyn and contribute to our understanding of myelin architecture at the molecular level.



Myelin is the lipid-rich multilamellar assembly of membrane processes extending from oligodendrocytes and Schwann cells, forming an insulating sheath around nerve axons in the central and peripheral nervous systems, respectively.¹ The myelin sheath is a dynamic system that communicates with both the underlying axon and the external environment and allows rapid transmission of nerve impulses by saltatory conduction.^{2,3} In the central nervous system (CNS, brain and spinal cord), the adhesion of the cytoplasmic surfaces of multilamellar internodal compact myelin is maintained by myelin basic protein (MBP), one of the two predominant proteins, the other being proteolipid protein (PLP). The classic (canonical) MBP isoforms range in nominal molecular mass from 14 to 21.5 kDa. The mutant line of *shiverer* mice lacks classic MBP isoforms because of an ablation of that portion of the gene; they have only one or two layers of poorly compacted myelin, which can be rescued by MBP-producing cells.⁴ Our focus here is on the most-studied 18.5 kDa MBP isoform,

which we shall henceforth simply call MBP, using murine sequence numbering unless otherwise noted (Figure 1).^{5,6} Because of its necessity for myelination, this MBP isoform has been called the “executive” protein of myelin.⁷ This protein interacts not only with membranes but also with calcium-activated calmodulin and SH3 domains and facilitates cytoskeletal assembly, as reviewed in refs 5, 6, and 8–14.

In this study, we have determined the NMR structure of residues S72–S107 of 18.5 kDa murine MBP in the presence of dodecylphosphocholine (DPC) micelles, as a membrane-mimetic condition that can be studied using solution spectroscopic approaches.^{15,16} There are two successive structural motifs within this region with different, but perhaps correlated, functionality. First, there is a membrane-associating

Received: July 25, 2012

Revised: August 31, 2012

Published: September 5, 2012



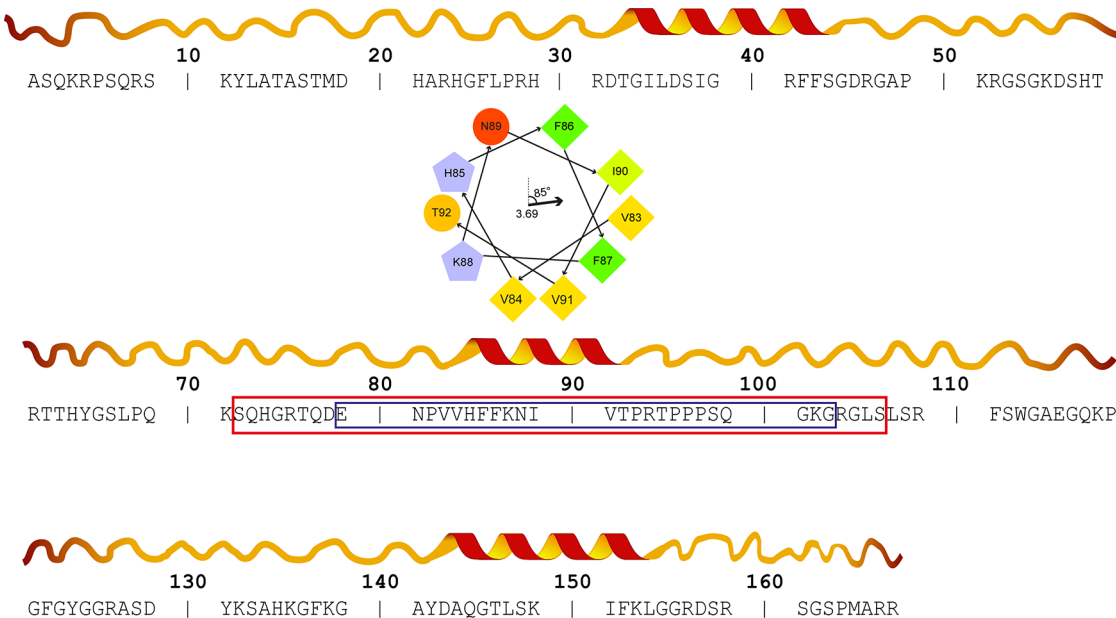


Figure 1. Residue road map of the murine classic 18.5 kDa MBP isoform (168 residues) showing the segments of interest. The helical wheel and overall hydrophobic moment vector of the central helical region (V83–T92) were produced using the DGwif interface scale.³² The residue types are coded by geometrical shapes: circles for hydrophilic, pentagons for potentially positively charged (e.g., His), and diamonds for hydrophobic. The hydrophobicity scale is color-coded with a red to yellow to green gradient, with the most hydrophobic residues colored green and the most hydrophilic red. The potentially charged residues are colored light blue. The overall hydrophobic moment value, vector, and angle are shown in the center of the wheel. The red rectangle outlines the S72–S107 α -peptide used for solution NMR spectroscopy *in vitro*, and the blue rectangle outlines the E80–G103 MD-peptide used for MD simulations *in silico*. The recombinant murine 18.5 kDa isoform studied previously by solution and solid-state NMR spectroscopy^{31,33} has an additional LEH₆ tag at the C-terminus.

amphipathic α -helix, comprising residues V83–T92 and representing an immunodominant epitope in multiple sclerosis. This motif has been studied experimentally by circular dichroism (CD), electron paramagnetic resonance (EPR), and solution and solid-state nuclear magnetic resonance (NMR) spectroscopy^{13,15,17–22} and has also been investigated by molecular modeling and molecular dynamics (MD) simulations.^{23,24} We emphasize that the spectroscopic studies were performed primarily on full-length recombinant murine 18.5 kDa MBP (rmMBP, 176 residues). Following this segment is a proline-rich segment considered to be an extended strand that can adopt a polyproline type II (PPII) conformation, as demonstrated by CD spectroscopy,^{5,25} and comprising a classic XP-x-XP SH3 domain recognition target. In studies performed with MBP both *in vitro* and *in vivo*, this motif of the protein has been shown to represent the target for SH3 domain-containing proteins such as Fyn.^{25–29}

We consider this central region of 18.5 kDa MBP (comprising the amphipathic membrane-anchoring α -helix and PPII SH3 ligand) to constitute a “molecular switch”³⁰ because of the number and variety of post-translational modifications that may represent different levels of control, particularly phosphorylation of residues T92 and T95 by mitogen-activated protein kinases (reviewed in refs 5, 6, 9, 10, and 12). This idea is supported by recent *in cellula* investigations in which transfection of an immortalized early developmental oligodendrocyte line by 18.5 kDa MBP variants, with proline substitutions and pseudophosphorylated threonines in this region, resulted in significant changes in cell morphology.²⁸ However, the structural changes of these modifications have yet to be elucidated. For these reasons, it is essential to study the conformations of this region of the protein, in physiologically relevant (membrane-associated)

environments. In general, MBP is a conformationally dynamic protein for which it is difficult to formulate an experimentally tractable membrane-mimetic system to probe its conformation in a straightforward manner at the amino acid level, e.g., by solution or solid-state NMR spectroscopy.^{5,6,9,13,16,22,31} For this reason, using a “divide-and-conquer” approach allows one to probe, in detail, the conformational variability of well-defined, individual portions of the protein. In particular, the fragment studied in this work should be an anchor point of the protein to the membrane; therefore, its structure should be independent of the rest of the protein, whose conformation strongly depends on the environment. Using the information collected in this study, along with data collected from other experiments (with both the full-length MBP, MD, and untagged peptide experiments), will provide a more complete picture of the conformation of MBP in membrane-mimetic environments. Here, we use established solution NMR spectroscopic approaches, complemented by MD simulations, as a step toward the overall goal of defining 18.5 kDa MBP’s conformation within the myelin sheath.

MATERIALS AND METHODS

Materials. Deuterated dodecylphosphocholine (DPC-*d*₃₈), ¹³C-labeled glucose, ¹⁵N-labeled NH₄Cl, and D₂O were purchased from Cambridge Isotope Laboratories (Cambridge, MA). All other chemicals were reagent grade or electrophoresis grade and were purchased from either Fisher Scientific (Unionville, ON) or Sigma-Aldrich (Oakville, ON).

Peptide Purification and Preparation for Solution NMR Spectroscopy. The segment of murine 18.5 kDa MBP coding for amino acids S72–S107 was cloned into the Champion pET SUMO (small ubiquitin modifier) Expression System (Invitrogen Life Technologies, Burlington, ON) and

Table 1. Summary of Solution NMR Acquisition Parameters

spectrum	no. of transients	carrier frequency (ppm)			sweep width (ppm)			no. of points			quadrature detection ^a	
		F ₁	F ₂	F ₃	F ₁	F ₂	F ₃	F ₁	F ₂	F ₃	F ₁	F ₂
HCAN	8	40	118	4.7	40	40	14	128	64	2048	S-TPPI	S-TPPI
HCCH	8	40	40	4.7	76	76	14	128	64	2048	S-TPPI	S-TPPI
HNCACB	8	40	118	4.7	76	35	14	144	44	2048	S-TPPI	S-TPPI
CBCA(CO)NH	8	40	118	4.7	76	35	14	144	44	2048	S-TPPI	S-TPPI
HNCO	16	175	118	4.7	25	35	14	72	44	2048	S-TPPI	S-TPPI
HN(CA)CO	16	175	118	4.7	25	35	14	72	44	2048	S-TPPI	S-TPPI
HSQC	10	115	4.7	—	30	16	—	128	2048	—	E-A-E	—

^aAbbreviations: S-TPPI, States-TPPI;³⁸ E-A-E, Echo-AntiEcho.³⁹

was named $\alpha 2$. This nomenclature arises from it being the second of three segments of 18.5 kDa MBP that form strongly amphipathic α -helices (Figure 1).^{5,6,32–34} The plasmid encoding this SUMO-MBP peptide fusion protein was transformed into *Escherichia coli* BL21-CodonPlus (DE3)-RP cells (Stratagene, La Jolla, CA), grown in M9 minimal medium supplemented with ¹³C-labeled glucose and ¹⁵N-labeled NH₄Cl, and was expressed and purified as introduced previously.³⁴ Using this system, we were able to express up to 130 mg of SUMO- $\alpha 2$ -peptide fused products per liter of culture and, using a native lysis procedure followed by immobilized metal affinity chromatography (using Ni-NTA resin), purify them from the whole bacterial lysates.³⁴ In the subsequent step, SUMO was enzymatically removed in the reaction with specific SUMO protease I (Ulp1, kindly provided by C. D. Lima, Sloan-Kettering Memorial Institute, New York, NY). To achieve complete cleavage, we applied 1 μ g of protease to 1 mg of fused proteins, and the reaction mixtures were incubated with protease at 30 °C for 3 h. The efficiency of proteolytic cleavage was assessed by Tricine-polyacrylamide gel electrophoresis (not shown), and the $\alpha 2$ -peptides were further purified by subtractive chromatography using the same Ni-NTA resin once again. During this chromatography step, the cleaved SUMO tag along with the SUMO protease bound to the column, because they both contained hexahistidine affinity tags, whereas the untagged $\alpha 2$ -peptides of interest were recovered in the flow-through and wash fractions. Peptides were further HPLC-purified, and the final purity was assessed by rechromatography by HPLC. The final purified product was diluted with Milli-Q water to <15% acetonitrile and frozen at –80 °C. At this point, the sample was lyophilized completely on a Labconco FreeZone freeze-dryer (Fisher Scientific, Markham, ON).

For reconstitution with DPC for solution NMR spectroscopy, approximately 2 mg of uniformly ¹³C- and ¹⁵N-labeled $\alpha 2$ -peptide was dissolved in 50 mM potassium phosphate buffer (pH 6.5), 10% D₂O, and 100 mM DPC-*d*₃₈. The sample was prepared according to the method of Shenkarev et al.³⁵ The total volume was brought to approximately 600 μ L, and the sample was transferred to a standard NMR tube and maintained at 285 K for all measurements. This temperature was chosen as it yielded the best peak resolution in two-dimensional ¹H-¹⁵N HSQC spectra.

Solution NMR Spectroscopy, Sequence-Specific Resonance Assignments, and Structure Calculations. The high-resolution ¹H, ¹³C, and ¹⁵N NMR spectra, using several complementary pulse sequences,³⁶ were recorded on a Bruker Avance spectrometer operating at a Larmor frequency of 600.13 MHz. In addition to the collection of (a) two-dimensional ¹H-¹⁵N HSQC spectra, the following triple-

resonance NMR experiments were performed to obtain residue-specific assignments: (b) HNCO/HN(CA)CO to assign the amide proton (¹H_N[i]), the amide nitrogen (¹⁵N[i]), and the carboxyl carbon atoms of the current and preceding amino acid (¹³C'[i], ¹³C'[i – 1]), (c) CBCA(CO)NH/HNCACB to assign the C_α and C_β atoms of the current and preceding amino acids, (d) HCCH-TOCSY (total correlation spectroscopy) to assign the remaining ¹H and ¹³C side chain atoms, and (e) HACAN to assign the prolyl residues.³⁷ Water suppression was achieved using the double-pulsed field gradient spin echo technique (excitation sculpting) with the carrier frequency set to the water ¹H signal. Detailed experimental spectroscopic parameters for all spectra are listed in Table 1.^{38,39}

The ¹H chemical shifts were referenced directly to the methyl signal of DSS (2,2-dimethylsilapentane-5-sulfonic acid) in an external sample tube, whereas the ¹³C and ¹⁵N chemical shifts were referenced to DSS indirectly. The spectra were processed using NMRPipe.⁴⁰ All field-induction decays were zero-filled and apodized using a shifted, squared sinusoidal bell function prior to Fourier transformation and subsequent phase correction. The HSQC spectrum was zero-filled up to 1024 and 4096 complex points along F₁ and F₂, respectively (Figure 2). Both HN(CA)CO and HNCACB spectra were zero-filled up to 512, 512, and 2048 complex points along F₁, F₂, and F₃, respectively (Figure 3). The HACAN spectrum was zero-filled up to 512, 512, and 2048 complex points along F₁, F₂, and F₃, respectively (Figure 4).

Spin systems were then assigned using Computer Assisted Resonance Assignment (CARA), version 1.8.4,⁴¹ modules contained in the CARA software package (<http://www.nmr.ch>), and a collection of in-house scripts that have been previously described.⁴² All spin systems were created on the basis of the ¹³C, ¹⁵N, and ¹H values (parts per million) of ¹³C'[i – 1], ¹⁵N[i], and ¹H_N[i] of each system in the HNCO spectrum. All other spin systems were picked and partially assigned automatically using another set of in-house scripts. Spin systems that were not identified by the scripts were assigned manually. Sequence-specific connectivity was obtained manually using iterative trials.

Secondary structure estimation by chemical shift index (CSI) analysis was performed as described previously (Figure 5).⁴³ In addition, we used the ¹³C_ω, ¹³C_β, ¹³C', ¹⁵N, ¹H_ω and ¹H_N assignments to produce structural models via ROSETTA (version 2.3.0) and CS-ROSETTA (version 1.01) calculations (Figure 6).⁴⁴ Molecular fragments were selected on the basis of the combined chemical shift information and amino acid sequence of the $\alpha 2$ -peptide (Figure 1). These fragments were then used to produce 10500 models using CS-ROSETTA. Residues S72–N81 and T92–S107 were excluded from the

CS-ROSETTA analysis, because CSI analysis identified those regions to be in a coil conformation. Models were averaged with XPLOR-NIH (version 2.31),^{45,46} and the *average.inp* script that looped through 10 input structures, and swapped them to minimize the final overall rmsd. The artifacts were eliminated with the help of energy minimization of the selected residues using the AMBER99 force field. Structures were generally rendered with PyMOL (The PyMOL Molecular Graphics System, version 1.5.0.4, Schrödinger, LLC, New York, NY).

Molecular Dynamics (MD) Simulations. The starting molecular model of the segment NH₃⁺-E⁸⁰NPVVHFFKNI⁹⁰VTPRTPPPSQ¹⁰⁰GKG¹⁰³-COO⁻ was constructed using Sybyl (version 7.0, Tripos Associates, St. Louis, MO) and was the same structure used by us previously.²⁴ Briefly, it comprised an amphipathic α -helix from residue E80 to residue V91 and an extended strand in a left-handed polyproline type II (PPII) conformation from residue T92 to residue G103. All prolyl residues were in the *trans* configuration.^{47,48} We henceforth refer to this *in silico* construct as the MD-peptide to distinguish it from the real, *in vitro*, α -peptide.

A pre-equilibrated micelle, comprising 65 dodecylphosphocholine (DPC) lysophospholipid molecules (the largest available), was downloaded from the site moose.bio.ucalgary.ca/index.php?page=Structures_and_Topologies at the University of Calgary (Calgary, AB).⁴⁹ The peptide model was positioned at the surface of the micelle, in an orientation in agreement with various functional and experimental data and hypotheses,^{5,15,19,24} and with the following electrostatic and hydrophobic characteristics: the hydrophobic surface, in particular the two Phe residues (F86 and F87) of the amphipathic α -helix, pointed down toward the hydrophobic tails, and the charged or polar residues pointed toward the polar headgroups or the solvent. The PPII structure was oriented outward with respect to the membrane, in the aqueous solvent.²⁴ The six lysophospholipid molecules that were present in a radius of 1 Å around the peptide were manually deleted.⁵⁰ The system was solvated with a layer of water molecules ~1.2 nm thick, with the addition of 1 nm in the y direction, to achieve better solvation of the PPII segment. Sodium and chloride ions were added to the aqueous layer of the system to obtain an overall zero charge and to reach a physiological salt concentration of 0.15 M.

The MD simulations were performed at Compute Canada/SharcNet facilities (<http://www.sharcnet.ca>) using the GROMACS (GROningen MACHine for Chemical Simulations) software package, version 4.0.5, and the Gromos96 ffG53a6 force field.⁵¹

Two MD simulations were performed, with the single histidyl residue in the MD-peptide (see Figure 1) in either the charged form or the neutral form. A short control simulation in an aqueous solution was initially run on the peptide with neutral N- and C-termini, and no difference in behavior was observed with respect to the zwitterionic form. We concluded that this latter form did not seem to influence the dynamics significantly, probably because of the presence of an oppositely charged residue at both N- and C-termini that partially shielded the net charges of the zwitterion. After an energy minimization of the whole system, a first position-restrained MD equilibration was performed keeping both the peptide and the DPC micelle fixed (100 ps); then a second equilibration was run keeping only the peptide fixed (1 ns). Periodic boundary conditions were applied to prevent random diffusion

of molecules outside the boundaries of the simulation box. The full MD simulations were run for 170 ns with the charged histidine and for 200 ns with the histidine in neutral form, at 300 K and 1 atm, with a time step of 2 fs. Temperature coupling was made using velocity rescaling with a stochastic term, with a time constant of 0.1 ps. The “protein+DPC” and “water+ions” groups were coupled separately to the temperature bath. The pressure coupling was isotropic, and the Berendsen barostat was used, with a coupling constant of 1 ps.

For visualization and analysis of structural files and trajectories computed by GROMACS, the GROMACS utilities and Visual Molecular Dynamics (VMD)⁵² were utilized.

Solution NMR Spectroscopy of the α 2-Peptide in Association with the Fyn-SH3 Domain. Another series of solution NMR experiments was conducted to observe how the chemical shifts of the α 2-peptide in solution were affected by introducing an MBP binding partner such as the Fyn-SH3 domain.²⁷ The plasmid encoding the *Gallus gallus* (chicken) SH3 domain of Fyn was a generous gift of A. Davidson (University of Toronto, Toronto, ON) and was expressed and purified as previously described.⁵³ Here, approximately 2 mg of α 2-peptide was dissolved in a HEPES buffer [20 mM HEPES, 100 mM NaCl, and 10% D₂O (pH 7.4)] to a total volume of 500 μ L. The Fyn-SH3 domain was also dissolved in the same buffer and titrated into the α 2-peptide solution to observe the chemical shift perturbations of the peptide in two-dimensional ¹H-¹⁵N HSQC spectra, at different α 2:Fyn-SH3 domain molar ratios (1:0, 1:0.2, 1:0.3, 1:0.5, 1:0.8, 1:0.9, 1:1, 1:1.1, and 1:1.2). Two additional samples of α 2-peptide were prepared to determine the chemical shift assignments of α 2-peptide/Fyn-SH3 solutions at 1:0 and 1:1 molar ratios in the buffer described here. The assignment method was the same as for the sample of the α 2-peptide in association with DPC.

■ RESULTS AND DISCUSSION

Background and Rationale. Previously, we have determined the structure of an 18-residue fragment of murine 18.5 kDa MBP (residues Q81-T98) in aqueous buffer, in 30% (v/v) trifluoroethanol, and in association with DPC micelles.¹⁵ We have also previously probed the conformation of this region by magic angle spinning solid-state NMR (ssNMR) spectroscopy, by selectively labeling valines and asparagines on full-length 18.5 kDa rmMBP (recombinant murine 18.5 kDa MBP), and using chemical shift indexing to observe the presence of secondary structural elements in the protein reconstituted with large unilamellar vesicles consisting of equimolar amounts of dimyristoylphosphatidylcholine and dimyristoylphosphatidylglycerol (DMPC/DMPG large unilamellar vesicles).²² The peptide structure revealed an amphipathic α -helical membrane-anchoring motif that had previously been identified in the full-length 18.5 kDa protein, at low resolution, by electron paramagnetic resonance spectroscopy.^{19,20} ssNMR spectroscopy revealed a tendency to form an α -helix between residues V83 and K88, based on the indexing of the Val and Asn C_α chemical shifts. Here, we will compare the chemical shifts of the α 2-peptide in the presence of DPC micelles to those of full-length 18.5 kDa rmMBP Val and Asn assignments in the presence of DMPC/DMPG large unilamellar vesicles, to assess the similarity of the chemical environments of those residues in the peptide and in full-length rmMBP, in somewhat different membrane-mimetic environments.

Adjacent to this α -helical segment is a proline-rich segment that is a classic binding target for SH3 domain-containing

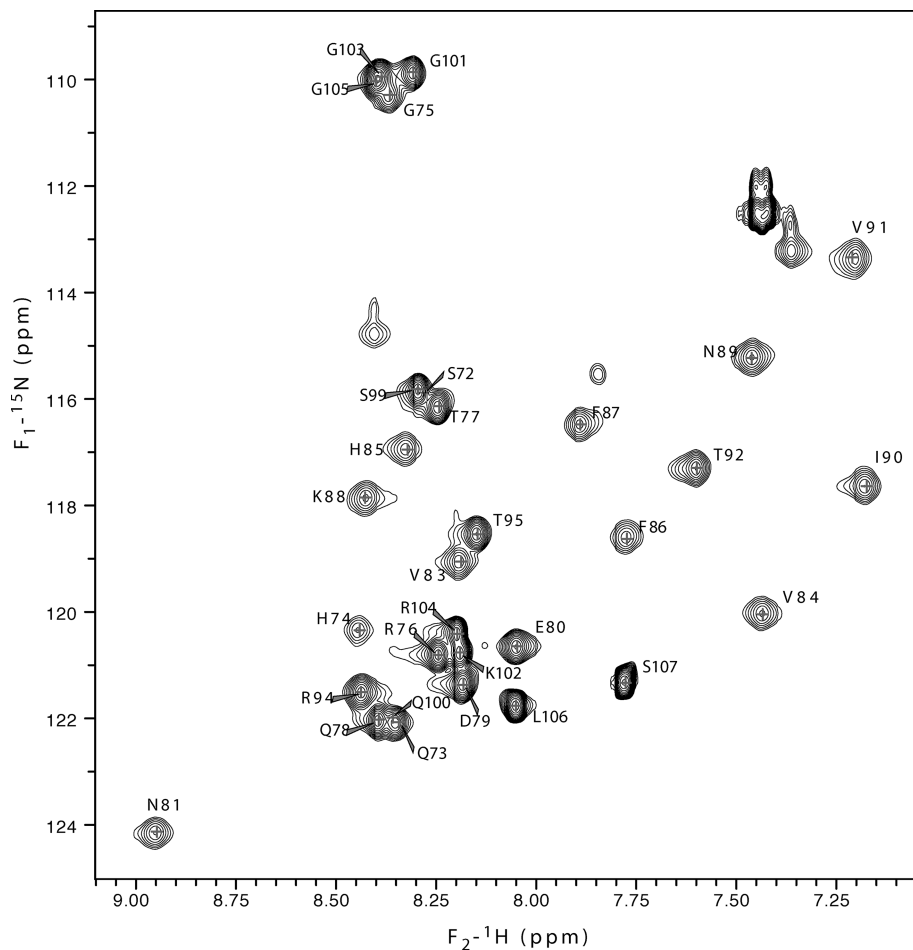


Figure 2. ^1H - ^{15}N HSQC spectrum of uniformly ^{13}C - and ^{15}N -labeled $\alpha 2$ -peptide (36 residues) dissolved in 50 mM potassium phosphate buffer (pH 6.5) and 10% D_2O , with 100 mM DPC- d_{38} , at a concentration of 1.47 mM, and recorded at 285 K. A total of 31 of 31 expected backbone peaks are assigned (there are five prolyl residues). The HSQC spectrum was processed by applying a 90°-shifted squared-sine bell function and zero-filled up to 1024 and 4096 complex points along F_1 and F_2 , respectively, prior to Fourier transformation using NMRPipe.

proteins such as Fyn tyrosine kinase.^{25,26,28,29} We have posited that the two motifs in juxtaposition constitute an essential interaction motif whose conformation is controlled by events such as phosphorylation, thereby affecting its function.^{5,6,24,28} This notion has analogous examples in other proteins such as tau.^{54,55} We have examined these ideas using MD simulations of the 24-residue MD-peptide comprising both motifs between residues E80 and G103 (murine 18.5 kDa MBP residue numbering), in association with an uncharged dimyristoylphosphatidylcholine (DMPC) bilayer, and have found a variety of conformational changes that may be relevant in vivo.²⁴ Here, we have extended these MD studies to determine experimentally the conformation of the considerably larger $\alpha 2$ -peptide comprising residues S72–S107 of this region of the protein, in association with DPC micelles, using solution NMR spectroscopy. The main reason is that DPC is a simple and effective membrane-mimetic system suitable for NMR studies of small polypeptides. The experimental work was complemented by MD simulations of the MD-peptide, comprising residues E80–G103, also in association with a DPC micelle *in silico*.

Peptide Purification and Preparation for Solution NMR Spectroscopy. The $\alpha 2$ -peptide (S72–S107) from the 18.5 kDa murine MBP amino acid sequence was designed initially to include one region of three (specifically V83–T92)

that are known to adopt a strongly amphipathic α -helical structure in association with detergent micelles and phospholipid bilayers.^{5,6,15,19,24} One of the methods for preventing *in vivo* degradation of recombinant short polypeptides during expression in prokaryotic cells (*E. coli*) is to express them as fusion proteins from which target peptides can be released by enzymatic cleavage. Here, we used a small ubiquitin-related modifier (SUMO) linked with a hexahistidine tag to over-express this MBP peptide in *E. coli* BL21-CodonPlus(DE3)-RP cells.³⁴ The purity of the $\alpha 2$ -peptide product was ~99%, and this protocol yielded ~13–18 mg of uniformly ^{13}C - and ^{15}N -labeled $\alpha 2$ -peptide per liter of culture.

Structure of the $\alpha 2$ -Peptide in Association with DPC Micelles. Dodecylphosphocholine (DPC) micelles (detergent with a critical micelle concentration of 1 mM) are a useful experimental mimic of membranes, particularly for focusing on segments of membrane-associated proteins such as 18.5 kDa MBP.^{15,16,34,56} Upon association with the lysophospholipid micelles, full-length MBP or peptide fragments thereof will undergo partial disorder-to-order transitions.^{5,6,13,34} Even under these conditions, however, the high degree of chemical shift degeneracy inherent to intrinsically disordered proteins (such as MBP) hinders resonance assignment, a problem compounded in HCN experiments by the high proportion of prolyl residues here in the $\alpha 2$ -peptide (see Figure 1). Fortunately,

some chemical shift resonances not only depend on amino acid type and its adopted secondary structure but also have strong sequence dependence. Examples of these resonances are the backbone amide nitrogen and carbonyl resonances. In our assignment strategy, we relied on this sequence dependence of carbonyl resonances to resolve the lack of dispersion in ^{15}N HSQC correlations resulting from the nature of the peptide under consideration. As a result, the ^1H , ^{15}N , and ^{13}C backbone assignments for this α 2-peptide were almost complete (Figure 2 and Table S1 of the Supporting Information).

Figure 3 shows strip plots of both HNCACB and HNC(CA)CO spectra, showing the advantage of using carbonyl resonances for determining the preceding spin system of G75 based on the different C'1 resonance in the overlapping region. Sequential connectivity along prolyl residues was achieved with the aid of HACAN.³⁷ In this experiment, the amide nitrogen atoms of the current (*i*) and following (*i* + 1) residues are correlated to both H_α and C_α of the current residue. An example of the assigned prolyl residues is given in Figure 4. Assignments of the aliphatic side chain ^{13}C and ^1H resonances were completed with the help of a HCCH-TOCSY analysis (spectrum not shown). The full resonance assignments are given in Table S1 of the Supporting Information and have been deposited in the Biological Magnetic Resonance Bank (BMRB, <http://www.bmrb.wisc.edu>) as entry 18520.

Chemical shift index analysis revealed some structural details (Figure 5). The central region of the α 2-peptide (P82–V91) shows a strong tendency to form an α -helix, as fully expected, whereas the rest of the α 2-peptide remains in a predominantly random coil conformation. These results were supported by CS-ROSETTA (version 1.01) analysis.

As a further means of identifying secondary structure elements using the chemical shifts found for the peptide, we input the chemical shifts into the δ 2D software designed by the Vendruscolo laboratory, and available on their web server.⁵⁷ This software calculates the probability that any amino acid in a disordered protein has a particular secondary structure conformation based on the chemical shift assignments, and the results for the α 2-peptide are listed in Table 2. The overall predictions for the α 2-peptide thus obtained were as follows: α -helix (H), 25.9%; extended β -strand (E), 2.3%; polyproline type II (PPII or P), 3.6%; coil (C), 68.3%. This method predicted the same α -helix length found in the CS-ROSETTA models, which illustrates the robustness of the latter analysis. Moreover, it defines the region forming the PPII structure, providing more information about the structural elements in this region determining this aspect of this protein's function.

We also compared the assignments of the α 2-peptide obtained here in DPC micelles to assignments previously obtained for the same region of full-length rmMBP in DMPC/DMPG large unilamellar vesicles by magic angle spinning ssNMR (Table 3). Interestingly, we observed that the chemical shifts for the Val and Asn residues are fairly well conserved (<1 ppm deviation between nuclei in the α 2-peptide in DPC micelles and rmMBP in DMPC/DMPG large unilamellar vesicles), for both the unmodified C1 and pseudodeiminated C8 charge variants previously studied.²² The similarity between the chemical shifts obtained in both studies shows that using peptides to probe the local conformational properties of 18.5 kDa MBP does have relevance to the full-length protein in situ. This congruence of results also supports the use of DPC as an appropriate membrane-mimetic environment, and that can yield results comparable to those of more complex

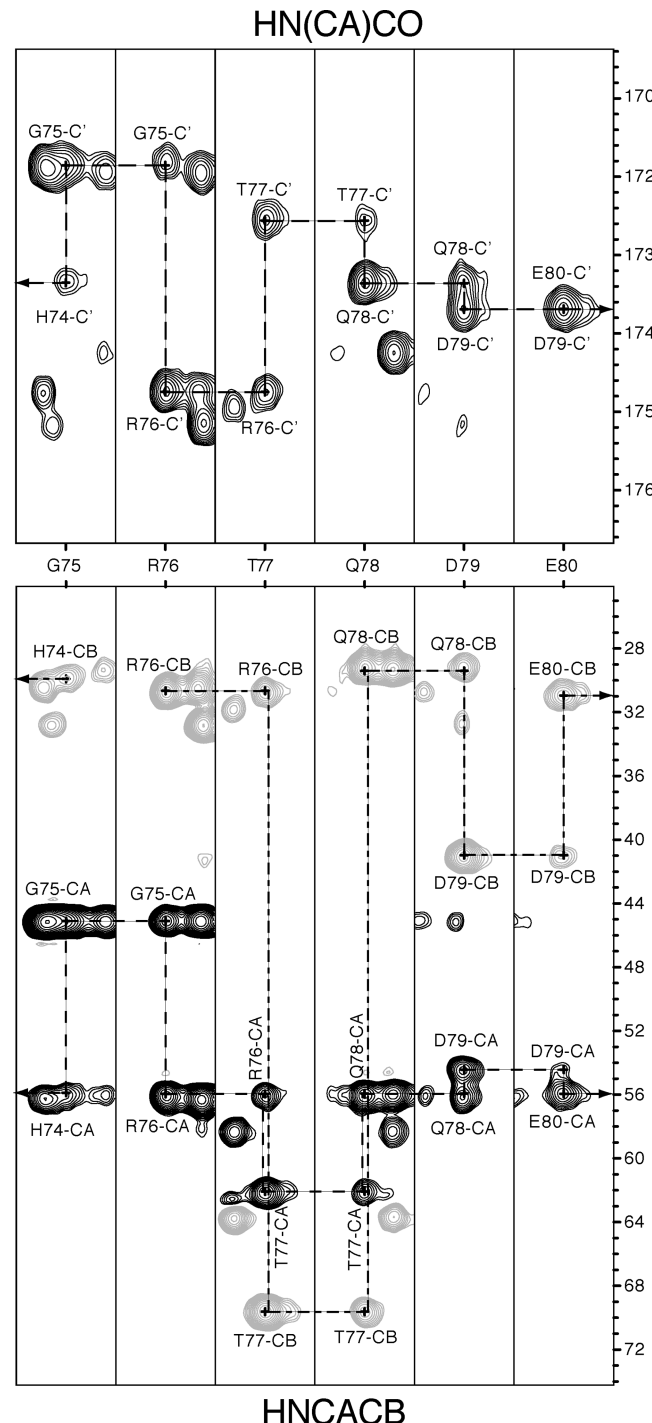


Figure 3. Establishing spin system connectivity based on the CO, Ca, and Cb resonances. The resonance overlap and spin system degeneracy were overcome by the help of dispersion of CO resonances due to sequence dependence, as exemplified in G75 and described in more detail in the text. Both HN(CA)CO and HNCACB spectra were processed by applying a 90°-shifted squared-sine bell window function and zero-filled up to 512, 512, and 2048 complex points along F_1 , F_2 , and F_3 , respectively, prior to Fourier transformation using NMRPipe.

phospholipid systems. The residue that shows the most deviation from ssNMR chemical shifts is N89. This residue had chemical shifts that were more suggestive of random coil than an α -helical conformation in full-length rmMBP, but in the α 2-peptide, the residue was part of a longer α -helix. These

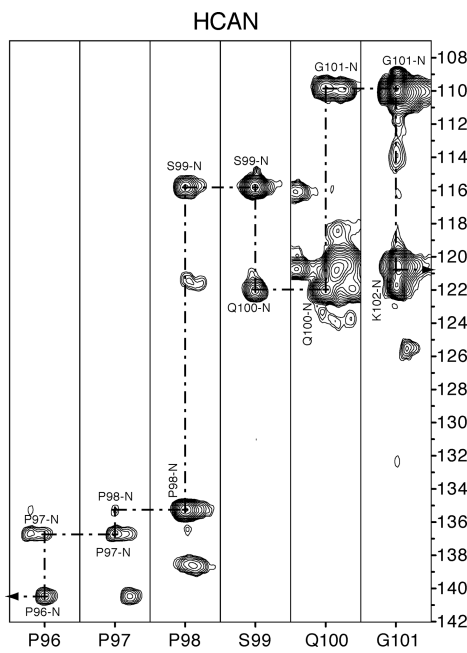


Figure 4. Prolyl residue assignment by HACAN spectroscopy.³⁷ This pulse sequence permits assignment of the prolyl amide nitrogen, because it does not require amide protons. It also allows for confirmation of assignments, because the C_α atom is coupled to $^{15}\text{N}[i]$ and $^{15}\text{N}[i+1]$. We used strips with assignments of residues P96–G101 to show the connectivity between residues, and the unique prolyl amide chemical shifts. The HACAN spectrum was processed by applying a 90°-shifted square-sine bell window function and zero-filled up to 512, 512, and 2048 complex points along F_1 , F_2 , and F_3 , respectively, prior to Fourier transformation using NMRPipe.

results were similar to what we have previously observed through EPR studies.^{19,20}

A comparison of the 1000 lowest-energy all atom models (obtained by CS-ROSETTA), based on the rmsd of the C_α chemical shifts, showed convergence around the lowest-energy model (Figure S1 of the Supporting Information). The 10 lowest-energy structures all show the presence of the central α -helical region, with high variability in fold in the N- and C-terminal regions of the α 2-peptide (Figure 6). This high mobility leads to a small number of NOE (nuclear Overhauser effect) constraints being detected along the α 2-peptide, and for this reason, we predicted the structure of the α 2-peptide using CS-ROSETTA. The models also show the mobile ends of the α 2-peptide folding toward each other, forming a network of hydrogen bonds. This phenomenon could be due to the length of the α 2-peptide, and the lack of the rest of the full-length MBP with other membrane-interacting motifs to help it maintain a more extended conformation between two membrane leaflets.^{16,33} On the other hand, a similar network of H-bonds may occur *in vivo* and contribute to the stabilization of the protein in a minimal hairpin conformation, with its two halves interacting separately with apposing membrane leaflets, as discussed in more detail elsewhere.^{22,24,58,59} The structural coordinates have been deposited in the Research Collaboratory for Structural Bioinformatics (RCSB) Protein Data Bank (PDB) (<http://www.rcsb.org>) as RCSB entry rcsb102847 and PDB entry 2lug.

Molecular Dynamics (MD) Simulations. Several MD simulations of the MD-peptide (E80–G103, murine 18.5 kDa MBP sequence numbering), corresponding to the highly

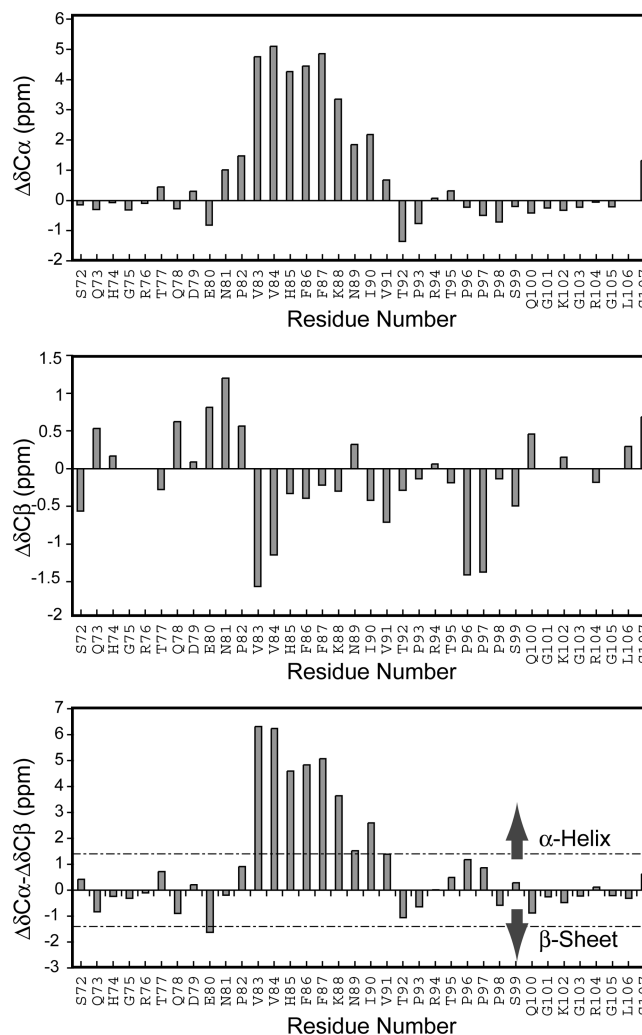


Figure 5. Secondary structure prediction of the α 2-peptide via standard chemical shift index analysis.⁴³

conserved central segment of the murine 18.5 kDa MBP fragment used for the NMR experiments (S72–S107), were performed to complement the NMR results. The starting model for the peptide comprises an α -helical region (residues E80–V91) followed by a segment in a PPII conformation (residues T92–G103), inserted at the micelle surface, as detailed above and previously.²⁴ This MD-peptide was shorter than the α 2-peptide, primarily because of the lack of structural information for the long N-terminal segment, which prohibits us from guessing at a starting structure for MD simulations. In addition, we can better compare the MD results in DPC with those obtained previously in a DMPC bilayer for the same peptide.²³ However, this choice focuses on the more interesting segment, which comprises the membrane-anchoring bound motif and the signaling protein binding target.

Two MD simulations using the histidyl residue both in the charged (170 ns simulation time) and in the neutral (200 ns simulation time) form were performed, to be in agreement with the pH value of 6.5 used in the NMR experiments. The two simulations led to the same stable structure [as we have observed by the rmsd plot during the trajectory (data not shown)], with a shortened α -helical region, anchored to the micelle by the hydrophobic surface residues, in particular by the two large F86 and F87 residues (Figures 7 and 8). During the

Table 2. Prediction of Secondary Structure Probabilities for Each Residue (populations per residue) in the α 2-Peptide, Using the Method of Camilloni et al. Designed for Disordered Proteins⁵⁷

residue	α -helix	β -strand	coil	PPII	prediction
S72					
Q73	0.004	0.035	0.959	0.001	C
H74	0.004	0.063	0.931	0.003	C
G75	0.003	0.084	0.908	0.004	C
R76	0.003	0.060	0.932	0.005	C
T77	0.003	0.029	0.965	0.003	C
Q78	0.003	0.011	0.985	0.002	C
D79	0.002	0.027	0.969	0.002	C
E80	0.074	0.049	0.871	0.005	C
N81	0.275	0.060	0.658	0.007	C
P82	0.594	0.043	0.357	0.006	H
V83	0.852	0.019	0.126	0.003	H
V84	0.977	0.003	0.019	0.001	H
H85	0.993	0.000	0.006	0.000	H
F86	0.988	0.000	0.012	0.000	H
F87	0.966	0.002	0.032	0.000	H
K88	0.925	0.004	0.071	0.000	H
N89	0.787	0.008	0.203	0.002	H
I90	0.558	0.010	0.426	0.007	H
V91	0.268	0.012	0.706	0.015	C
T92	0.087	0.010	0.883	0.020	C
P93	0.014	0.009	0.956	0.021	C
R94	0.017	0.012	0.915	0.057	C
T95	0.026	0.025	0.790	0.158	C
P96	0.057	0.039	0.631	0.273	C
P97	0.081	0.045	0.597	0.277	C
P98	0.093	0.031	0.714	0.162	C
S99	0.058	0.018	0.872	0.052	C
Q100	0.028	0.011	0.949	0.012	C
G101	0.009	0.011	0.956	0.024	C
K102	0.011	0.006	0.947	0.036	C
G103	0.012	0.006	0.953	0.030	C
R104	0.012	0.008	0.965	0.016	C
G105	0.011	0.012	0.972	0.005	C
L106	0.009	0.012	0.977	0.003	C
S107					

trajectory, the originally extended PPII region starts to bend at the P93 residue (Figure 7), partially unfolding the C-terminus of the α -helix. This disposition is favored by the geometrical hindrance of the proline side chain. Because the N-terminus of the α -helix unravels partially, only the central (H85–I90) residues remain in a fully α -helical conformation. The PPII segment bends toward the micelle, dragged by the hydrophobic residues (in particular, the prolines) that interact with the detergent hydrophobic tails and by the polar and charged residues that interact with the phosphate groups of the polar heads.

Two inter-related questions that have been addressed in the past have been whether a single molecule of 18.5 kDa MBP can bring two apposing leaflets of the oligodendrocyte membrane close to each other, with two halves of the protein associated with different myelin membrane leaflets,^{22,24,58,59} and whether the protein has a tertiary conformation akin to a molten globule,^{5,6,60} i.e., an ensemble with loose tertiary contacts.^{61,62} An early study on 18.5 kDa MBP had questioned whether the triproline repeat (murine residues P96, P97, and P98) formed a

Table 3. Comparison of Chemical Shift Assignments of the α 2-Peptide Reconstituted with DPC Micelles to ssNMR Assignments of Valyl and Asparaginyl Residues of Full-Length 18.5 kDa rmMBP Reconstituted with DMPC/DMPG Large Unilamellar Vesicles^a

nucleus	MBP isoform (ppm)			difference (ppm)		
	α 2	C1	C8	α 2 – C1	C1 – C8	α 2 – C8
N81 C_{α}	51.9	52.1	52.4	−0.2	−0.3	−0.5
N81 C_{β}	39.4	39.9	40.1	−0.5	−0.2	−0.7
V83 C_{α}	66.3	66.3	66.3	0.0	0.0	0.0
V83 C_{β}	31.1	31.3	31.4	−0.2	−0.1	−0.3
V84 C_{α}	66.8	67.0	66.8	−0.2	0.2	0.0
V84 C_{β}	31.5	31.9	31.8	−0.4	0.1	−0.3
N89 C_{α}	54.5	52.9	53.5	1.6	−0.6	1.0
N89 C_{β}	38.5	40.3	40.4	−1.8	−0.1	−1.9
V91 C_{α}	62.2	62.3	62.3	−0.1	0.0	−0.1
V91 C_{β}	32.2	32.1	32.3	0.1	−0.2	−0.1

^aData from ref 22. C1 refers to the unmodified rmMBP charge component and C8 to the pseudodeiminated rmMBP charge component, with net positive charges of +19 and +13, respectively, at neutral pH.

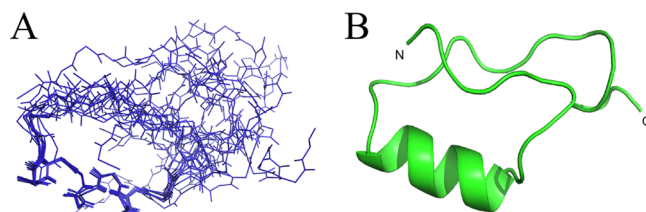


Figure 6. Structure calculation using CS-ROSETTA. (A) Superimposition of the 10 lowest-energy CS-ROSETTA models of the α 2-peptide. (B) Cartoon schematic of an average structure produced from the 10 lowest-energy α 2-peptide models.

bend and found that it did not.⁴⁸ Here, we see that the bend occurs at P93 instead. This structural feature could contribute minimally to a hairpin model of MBP in which N- and C-termini interact with separate membrane leaflets, as discussed in detail elsewhere.^{22,24,58,59} We had previously observed a sharp bend at this residue in our recent MD simulations of the MD-peptide on a DMPC bilayer²⁴ but here present direct experimental evidence.

Comparison of MD with NMR Results. A complement of the NMR results with MD simulations is useful for gaining insight into the mechanisms of peptide–lipid interactions that cannot be easily revealed by NMR experiments alone. To compare the structures obtained from the NMR experiments and the MD simulations, we made a superimposition starting from the supposition that the α -helical region should assume the same orientation with respect to the micelle surface.^{15,19,20,22} In both structures, the bend at residue P93 is present, in agreement with our hypothesis about its structural role in the myelin membrane.^{5,6,23,24}

Instead, the more evident difference is that the PPII region in the NMR structure is very flexible (Figures 6 and 8) and more solvent-exposed. In comparison, in the MD structure, the PPII segment is wrapped around the micelle. However, we must emphasize that the NMR α 2-peptide has two longer and flexible regions at the ends of the α -helix that are able to interact with each other, forming several H-bonds that stabilize a “closed” conformation (Figure 8). The MD-peptide, instead,

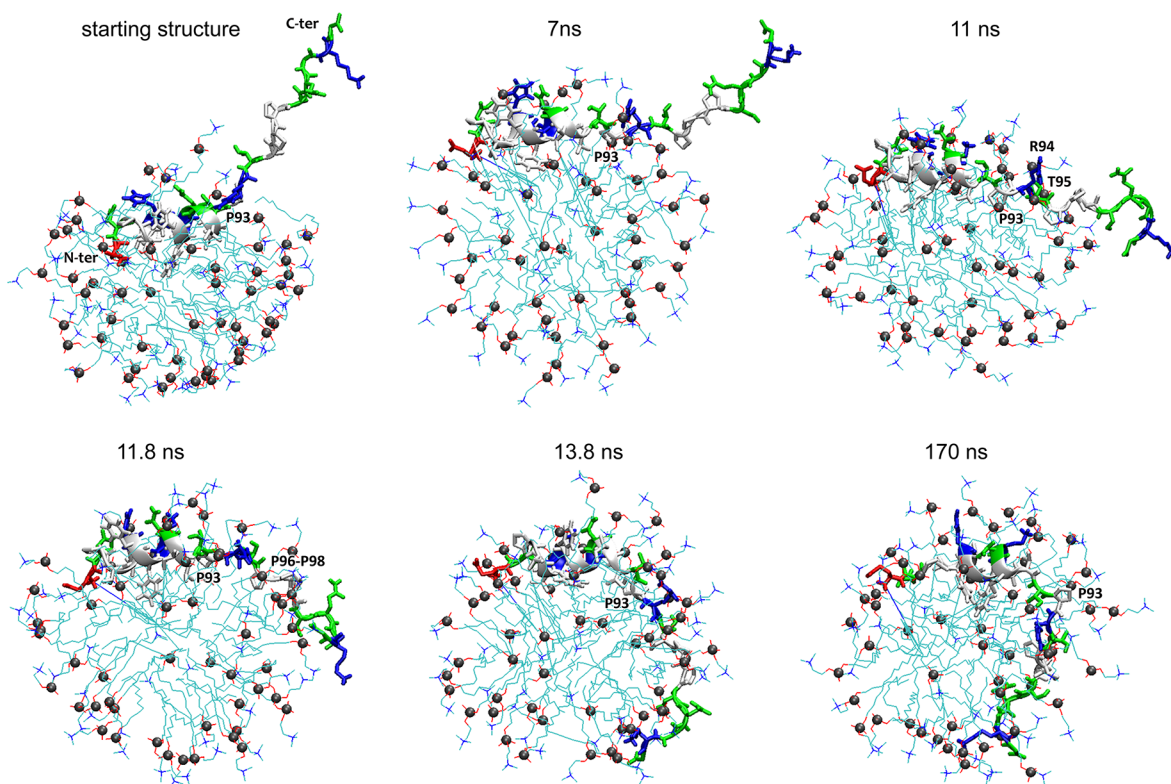


Figure 7. Selected snapshots of the MD trajectory of the E80–G103 MD-peptide showing the bending of the PPII tail. The peptide, in a cartoon–stick representation, is colored by residue type (white, hydrophobic; green, polar; blue, basic; red, acidic). The lysophospholipids of the micelle are depicted as thin sticks, colored by element; the dark gray spheres represent the phosphorus atoms of the lysophospholipid headgroups. The snapshots show the main steps of the adhesion of the PPII tail to the micelle, which takes place very quickly (<15 ns). The bending at residue P93 (7 ns) drags the rest of the chain. The charged R94 and polar T95 side chains interact with the lysophospholipid polar headgroups (11 ns). Then the three prolines (residues 96–98) penetrate, as does residue P93, among the lysophospholipid tails (11.8 ns). Finally, the C-terminal polar and charged residues adhere to the micelle surface (13.8 ns). The final conformation (170 ns) shows the PPII chain wrapped around the micelle.

has only the PPII segment that forms more favorable interactions with the micelle than the solvent, probably satisfying better both the hydrophobic and the polar nature of its residues. This fact is also confirmed by the behavior observed during the trajectory in the DMPC bilayer,²⁴ in which the oscillating PPII segment showed additional conformations lying down on the membrane surface. In addition, we have to consider the size of the *in silico* micelle (65 DPC molecules) with respect to the peptide length. In the final conformation obtained by MD simulation, it does not allow the whole α -helix to penetrate deeply into the micelle, letting the bend at the P93 residue generate the wrapped disposition of the PPII segment (Figure 7).

It is probably for the same reason that the shallower micelle penetration of the two extremities of the α -helical segment makes them less stable, and the α -helix slightly shorter in the MD-derived structure than in the NMR-derived one (MD residues H84–I90 and NMR residues P82–V91). In fact, it is also shorter than in the MD-derived structure performed previously on the E80–G103 MD-peptide in association with a DMPC bilayer (residues N81–V91).²⁴ In addition, the greater fluidity of a micelle system with respect to a bilayer is known to make the protein component more flexible.⁶³

These considerations underline the relevance of the membrane depth penetration on the length and stability of this amphipathic α -helix, as was previously revealed in EPR and solid-state NMR studies of the exposure of this α -helix to the solvent on the pseudodeiminated, membrane-bound, full-length

18.5 kDa MBP.^{20,22} This latter variant of the protein, as occurs in increased proportion in multiple sclerosis, has a reduced net positive charge compared to the unmodified form studied here, which contributes to myelin destabilization and disruption.⁶⁴ We are presently using this refined experimental model of this central segment of 18.5 kDa MBP to study the effects of phosphorylation of the two constituent threonyl residues (T92 and T95), as occurs *in vivo* by mitogen-activated protein kinases.^{5,6,9} These modifications have already been shown to have phenotypic changes *in cellula*²⁸ and would be expected to have synergistic, functional effects on the structure of the protein in this region, and on its association with both the lipid bilayer and SH3 domains such as that of Fyn.

Solution NMR Spectroscopy of the α 2-Peptide in Association with the Fyn-SH3 Domain. We have also titrated Fyn-SH3 into a solution of the α 2-peptide to probe the interaction between these binding partners (Figure S2 of the Supporting Information).²⁷ The titration of Fyn-SH3 into a solution of fully ^{13}C - and ^{15}N -labeled α 2-peptide showed chemical shift perturbations of several assigned regions (Figure 9). The most pronounced perturbations throughout the titration were assigned to non-prolyl residues in the proline-rich region of the α 2-peptide, suggesting that this is in fact the point at which Fyn-SH3 and the α 2-peptide are interacting. A more detailed study of the mode of interaction between Fyn-SH3 and MBP is currently underway in our laboratory.

Assessment of DPC Micelles for Studying 18.5 kDa MBP. The myelin sheath of the central nervous system is

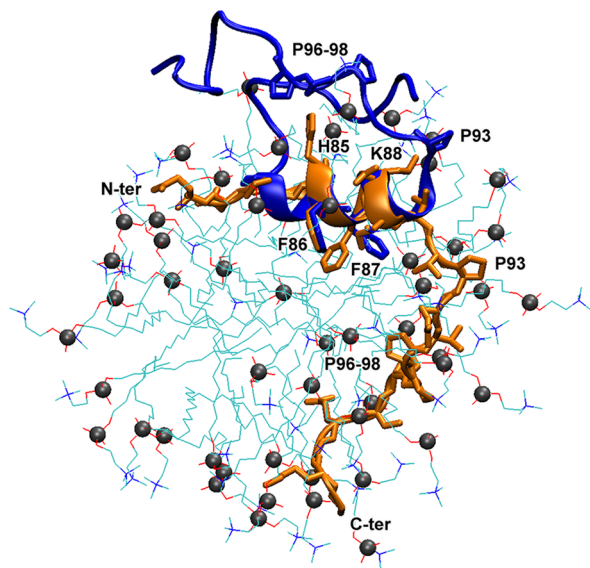


Figure 8. Superimposition of the average structure produced from the 10 lowest-energy models of the S72–S107 α 2-peptide (blue) with the conformation of the E80–G103 MD-peptide (orange) obtained after a 170 ns MD simulation in DPC (charged histidines). The orientation of the NMR structure with respect to the micelle is presumed to be the same as that obtained by MD, as previously determined with a smaller peptide using paramagnetic agents.¹⁵ The two anchoring residues (F86 and F87), the “snorkeling” K88 and H85 ones, and the bent P93 are labeled, as well as the three consecutive prolyl residues. The color scheme of the lysophospholipids of the micelle is as in Figure 7.

compositionally complex and difficult to study at high resolution except in highly reduced systems. Solid-state magic angle spinning NMR spectroscopy has been performed on full-length, uniformly ^{13}C - and ^{15}N -labeled 18.5 kDa MBP reconstituted in DMPC/DMPG bilayers.³¹ The synthetic phospholipids were required because of their stability over the prolonged course of NMR spectral collection. The results indicated that a considerable proportion (roughly one-third) of the protein was mobile and exposed to solvent, making its analysis considerably more complex than, say, that of transmembrane α -helical domains that are more commonly being studied in this manner. Clearly, complementary solid-state NMR spectroscopic and MD simulations of the full-length 18.5 kDa MBP, reconstituted in truly myelin-mimetic membrane systems, remain a relatively long-term goal.

At present, the DPC micelle system represents a reasonable nexus for investigations using complementary techniques for cross-validation.⁶⁵ This system is a useful membrane model for the study of small peptides such as those derived from MBP,¹⁵ is suitable for solution NMR spectroscopic experiments with them (cf, ref 16), and is still of acceptable computational burden for MD simulations. That is why it is so ubiquitous (e.g., refs 66–69). One caveat to note is the micelle’s small dimensions (even if we use the largest one available for MD simulations). In particular, the small bend radius becomes relevant if we study longer peptides interacting at the micelle’s surface, as we have done here. Nevertheless, this work is an essential step toward the far more challenging goals of elucidation of the structure of segments of 18.5 kDa MBP,

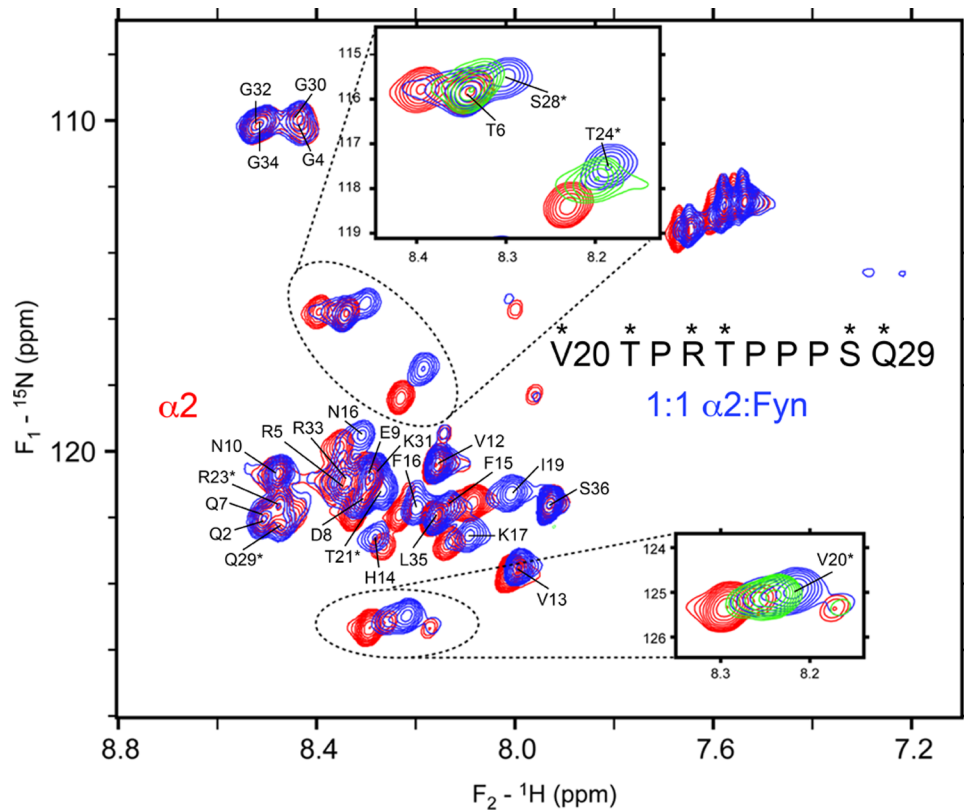


Figure 9. $^1\text{H}-^{15}\text{N}$ HSQC spectrum showing the chemical shift perturbations of the α 2-peptide (red) in the presence of an equimolar amount of the SH3 domain of Fyn (blue). Intermediate 1:0.5 molar ratios are shown for certain chemical shifts (green). All assignments shown are based on the 1:1 α 2-peptide:Fyn-HSQC spectrum.

and eventually the entire protein, under myelin-mimetic conditions using solid-state NMR spectroscopy.^{13,22,31,70}

CONCLUDING REMARKS

The classic isoforms of MBP are highly conserved in sequence in mammals, especially the central fragment studied here, comprising membrane association and protein association motifs in tandem. The structural importance of this region lies in its bend, possibly imparting upon the protein the ability to interact with two separate leaflets of the myelin membrane simultaneously. Its functional importance lies in its association both with the membrane and with proteins such as Fyn tyrosine kinase. The effects of phosphorylation of the threonyl residues in the SH3 ligand on both the local membrane association and the stability of the constituent secondary structural motifs are currently being studied in our laboratory.

ASSOCIATED CONTENT

Supporting Information

A plot showing rescored CS-ROSETTA all atom energies of 1000 models, compared to the rmsd of the C_α chemical shifts relative to the lowest-energy structure (Figure S1), strip plots of spectra used for assignment of the α 2-peptide shifts in the presence of an equimolar amount of the Fyn-SH3 domain (Figure S2), and the ^1H , ^{13}C , and ^{15}N chemical shifts of the α 2-peptide, referenced to DSS (4,4-dimethyl-4-silapentane-1-sulfonic acid) (Table S1), which have been deposited in the Biological Magnetic Resonance Bank as entry 18520. This material is available free of charge via the Internet at <http://pubs.acs.org>.

AUTHOR INFORMATION

Corresponding Author

*Department of Molecular and Cellular Biology, University of Guelph, 50 Stone Rd. E., Guelph, Ontario N1G 2W1, Canada. E-mail: gharauz@uoguelph.ca. Fax: (519) 837-1802. Telephone: (519) 824-4120, ext. 52535.

Author Contributions

M.A.M.A. and M.D.A. contributed equally to this work.

Funding

This work was supported by the Natural Sciences and Engineering Research Council of Canada (RG121541 to G.H.). M.D.A. and V.V.B. were recipients of a Doctoral Studentship and a Postdoctoral Fellowship, respectively, from the Multiple Sclerosis Society of Canada.

Notes

The authors declare no competing financial interest.

ACKNOWLEDGMENTS

The MD simulations were made possible by the facilities of the Shared Hierarchical Academic Research Computing Network (SHARCNET, <http://www.sharcnet.ca>) and Compute/Canada. The pET28b plasmid encoding recombinant SUMO protease, His-tagged Ulp(403–621), was a kind gift from Dr. Christopher Lima (Sloan-Kettering Memorial Institute). The plasmid encoding the *Gallus gallus* (chicken) Fyn-SH3 domain was a kind gift from Dr. Alan Davidson (University of Toronto). We are grateful to Ms. Valerie Robertson and Mr. Peter Scheffer (University of Guelph NMR Centre, Guelph, ON) and to Mrs. Janine Voyer-Grant for superb technical support. We thank Dr. Joan Boggs (University of Toronto), Dr. Vladimir Ladizhansky (University of Guelph, Guelph, ON),

and Dr. Kenrick Vassall (University of Guelph) for helpful discussions and comments on the manuscript.

ABBREVIATIONS

CARA, computer-aided resonance assignment; CNS, central nervous system; CSI, chemical shift index(ing); DMPC, dimyristoylphosphatidylcholine; DMPG, dimyristoylphosphatidylglycerol; DPC, dodecylphosphocholine; DSS, 2,2-dimethylsilapentane-5-sulfonic acid; HPLC, high-performance liquid chromatography; HSQC, heteronuclear single-quantum coherence; MBP, myelin basic protein; MD, molecular dynamics; NOE, nuclear Overhauser effect; rmMBP, 18.5 kDa recombinant murine MBP (A1-R168-Leu-Glu-His₆); rmsd, root-mean-squared deviation; SH3, Src homology 3; SUMO, small ubiquitin modifier; TOCSY, total correlation spectroscopy.

REFERENCES

- (1) Baumann, N., and Pham-Dinh, D. (2001) Biology of oligodendrocyte and myelin in the mammalian central nervous system. *Physiol. Rev.* 81, 871–927.
- (2) Piaton, G., Gould, R. M., and Lubetzki, C. (2010) Axon-oligodendrocyte interactions during developmental myelination, demyelination and repair. *J. Neurochem.* 114, 1243–1260.
- (3) Sty, P. K. (2011) The axo-myelinic synapse. *Trends Neurosci.* 34, 393–400.
- (4) Windrem, M. S., Nunes, M. C., Rashbaum, W. K., Schwartz, T. H., Goodman, R. A., McKhann, G., Roy, N. S., and Goldman, S. A. (2004) Fetal and adult human oligodendrocyte progenitor cell isolates myelinate the congenitally dysmyelinated brain. *Nat. Med.* 10, 93–97.
- (5) Harauz, G., and Libich, D. S. (2009) The classic basic protein of myelin: Conserved structural motifs and the dynamic molecular barcode involved in membrane adhesion and protein-protein interactions. *Curr. Protein Pept. Sci.* 10, 196–215.
- (6) Harauz, G., Ladizhansky, V., and Boggs, J. M. (2009) Structural polymorphism and multifunctionality of myelin basic protein. *Biochemistry* 48, 8094–8104.
- (7) Moscarello, M. A. (1997) Myelin basic protein, the “executive” molecule of the myelin membrane. In *Cell Biology and Pathology of Myelin: Evolving Biological Concepts and Therapeutic Approaches* (Juurlink, B. H. J., Devon, R. M., Doucette, J. R., Nazarali, A. J., Schreyer, D. J., and Verge, V. M. K., Eds.) pp 13–25, Plenum Press, New York.
- (8) Smith, R. (1992) The basic protein of CNS myelin: Its structure and ligand binding. *J. Neurochem.* 59, 1589–1608.
- (9) Harauz, G., Ishiyama, N., Hill, C. M. D., Bates, I. R., Libich, D. S., and Farès, C. (2004) Myelin basic protein: Diverse conformational states of an intrinsically unstructured protein and its roles in myelin assembly and multiple sclerosis. *Micron* 35, 503–542.
- (10) Boggs, J. M. (2006) Myelin basic protein: A multifunctional protein. *Cell. Mol. Life Sci.* 63, 1945–1961.
- (11) Harauz, G., and Musse, A. A. (2007) A tale of two citrullines: Structural and functional aspects of myelin basic protein demyelination in health and disease. *Neurochem. Res.* 32, 137–158.
- (12) Boggs, J. M. (2008) *Myelin Basic Protein*, Nova Science Publishers, Hauppauge, NY.
- (13) Libich, D. S., Ahmed, M. A. M., Zhong, L., Bamm, V. V., Ladizhansky, V., and Harauz, G. (2010) Fuzzy complexes of myelin basic protein: NMR spectroscopic investigations of a polymorphic organizational linker of the central nervous system. *Biochem. Cell Biol.* 88 (Special Issue on Protein Folding:Principles and Diseases), 143–155.
- (14) Simons, M., Snaidero, N., and Aggarwal, S. (2012) Cell polarity in myelinating glia: From membrane flow to diffusion barriers. *Biochim. Biophys. Acta* 1821, 1146–1153.
- (15) Farès, C., Libich, D. S., and Harauz, G. (2006) Solution NMR structure of an immunodominant epitope of myelin basic protein.

- Conformational dependence on environment of an intrinsically unstructured protein. *FEBS J.* 273, 601–614.
- (16) Libich, D. S., and Harauz, G. (2008) Solution NMR and CD spectroscopy of an intrinsically disordered, peripheral membrane protein: Evaluation of aqueous and membrane-mimetic solvent conditions for studying the conformational adaptability of the 18.5 kDa isoform of myelin basic protein (MBP). *Eur. Biophys. J.* 37, 1015–1029.
- (17) Whitaker, J. N., Moscarello, M. A., Herman, P. K., Epand, R. M., and Surewicz, W. K. (1990) Conformational correlates of the epitopes of human myelin basic protein peptide 80–89. *J. Neurochem.* 55, 568–576.
- (18) Bates, I. R., Boggs, J. M., Feix, J. B., and Harauz, G. (2003) Membrane-anchoring and charge effects in the interaction of myelin basic protein with lipid bilayers studied by site-directed spin labeling. *J. Biol. Chem.* 278, 29041–29047.
- (19) Bates, I. R., Feix, J. B., Boggs, J. M., and Harauz, G. (2004) An immunodominant epitope of myelin basic protein is an amphipathic α -helix. *J. Biol. Chem.* 279, 5757–5764.
- (20) Musse, A. A., Boggs, J. M., and Harauz, G. (2006) Deimination of membrane-bound myelin basic protein in multiple sclerosis exposes an immunodominant epitope. *Proc. Natl. Acad. Sci. U.S.A.* 103, 4422–4427.
- (21) Boggs, J. M., Bates, I. R., Musse, A. A., and Harauz, G. (2008) Interactions of the 18.5 kDa myelin basic protein with lipid bilayers: Studies by electron paramagnetic resonance spectroscopy and implications for generation of autoimmunity in multiple sclerosis. In *Myelin Basic Protein* (Boggs, J. M., Ed.) pp 105–125, Nova Science Publishers, New York.
- (22) Ahmed, M. A. M., Bamm, V. V., Harauz, G., and Ladizhansky, V. (2010) Solid-state NMR spectroscopy of membrane-reconstituted myelin basic protein: Conformation and dynamics of an immunodominant epitope. *Biophys. J.* 99, 1247–1255.
- (23) Bessonov, K., Bamm, V. V., and Harauz, G. (2010) Misincorporation of the proline homologue Aze (azetidine-2-carboxylic acid) into recombinant myelin basic protein. *Phytochemistry* 71, 502–507.
- (24) Polverini, E., Coll, E. P., Tieleman, D. P., and Harauz, G. (2011) Conformational choreography of a molecular switch region in myelin basic protein: Molecular dynamics shows induced folding and secondary structure type conversion upon threonyl phosphorylation in both aqueous and membrane-associated environments. *Biochim. Biophys. Acta* 1808, 674–683.
- (25) Polverini, E., Rangaraj, G., Libich, D. S., Boggs, J. M., and Harauz, G. (2008) Binding of the proline-rich segment of myelin basic protein to SH3-domains: Spectroscopic, microarray, and modelling studies of ligand conformation and effects of post-translational modifications. *Biochemistry* 47, 267–282.
- (26) Homchaudhuri, L., Polverini, E., Gao, W., Harauz, G., and Boggs, J. M. (2009) Influence of membrane surface charge and post-translational modifications to myelin basic protein on its ability to tether the Fyn-SH3 domain to a membrane *in vitro*. *Biochemistry* 48, 2385–2393.
- (27) De Avila, M., Ahmed, M. A. M., Smith, G. S. T., Boggs, J. M., and Harauz, G. (2011) Modes of SH3-domain interactions of 18.5 kDa myelin basic protein *in vitro* and in oligodendrocytes. Biophysical Society-55th Annual Meeting, March 5–9, 2011, Abstract B164.
- (28) Smith, G. S. T., De Avila, M., Paez, P. M., Spreuer, V., Wills, M. K., Jones, N., Boggs, J. M., and Harauz, G. (2012) Proline substitutions and threonine pseudophosphorylation of the SH3 ligand of 18.5-kDa myelin basic protein decrease its affinity for the Fyn-SH3 domain and alter process development and protein localization in oligodendrocytes. *J. Neurosci. Res.* 90, 28–47.
- (29) Smith, G. S. T., Homchaudhuri, L., Boggs, J. M., and Harauz, G. (2012) Classic 18.5- and 21.5-kDa myelin basic protein isoforms associate with cytoskeletal and SH3-domain proteins in the immortalized N19-oligodendroglial cell line stimulated by phorbol ester and IGF-1. *Neurochem. Res.* 37, 1277–1295.
- (30) Van Roey, K., Gibson, T. J., and Davey, N. E. (2012) Motif switches: Decision-making in cell regulation. *Curr. Opin. Struct. Biol.* 22, 378–385.
- (31) Zhong, L., Bamm, V. V., Ahmed, M. A., Harauz, G., and Ladizhansky, V. (2007) Solid-state NMR spectroscopy of 18.5 kDa myelin basic protein reconstituted with lipid vesicles: Spectroscopic characterisation and spectral assignments of solvent-exposed protein fragments. *Biochim. Biophys. Acta* 1768, 3193–3205.
- (32) Wimley, W. C., and White, S. H. (1996) Experimentally determined hydrophobicity scale for proteins at membrane interfaces. *Nat. Struct. Biol.* 3, 842–848.
- (33) Libich, D. S., and Harauz, G. (2008) Backbone dynamics of the 18.5 kDa isoform of myelin basic protein reveals transient α -helices and a calmodulin-binding site. *Biophys. J.* 94, 4847–4866.
- (34) Bamm, V. V., De Avila, M., Smith, G. S. T., Ahmed, M. A., and Harauz, G. (2011) Structured functional domains of myelin basic protein: Cross talk between actin polymerization and Ca^{2+} -dependent calmodulin interaction. *Biophys. J.* 101, 1248–1256.
- (35) Shenkarev, Z. O., Balashova, T. A., Efremov, R. G., Yakimenko, Z. A., Ovchinnikova, T. V., Raap, J., and Arseniev, A. S. (2002) Spatial structure of zervamicin IIB bound to DPC micelles: Implications for voltage-gating. *Biophys. J.* 82, 762–771.
- (36) Sattler, M., Schleucher, J., and Griesinger, C. (1999) Heteronuclear multidimensional NMR experiments for the structure determination of proteins in solution employing pulsed field gradients. *Prog. Nucl. Magn. Reson. Spectrosc.* 34, 93–158.
- (37) Kanelis, V., Donaldson, L., Muhandiram, D. R., Rotin, D., Forman-Kay, J. D., and Kay, L. E. (2000) Sequential assignment of proline-rich regions in proteins: Application to modular binding domain complexes. *J. Biomol. NMR* 16, 253–259.
- (38) Marion, D., Ikura, M., Tschudin, R., and Bax, A. (1989) Rapid recording of 2D NMR spectra without phase cycling: Application to the study of hydrogen-exchange in proteins. *J. Magn. Reson.* 85, 393–399.
- (39) Kay, L. E., Keifer, P., and Saarinen, T. (1992) Pure absorption gradient-enhanced heteronuclear single quantum correlation spectroscopy with improved sensitivity. *J. Am. Chem. Soc.* 114, 10663–10665.
- (40) Delaglio, F., Grzesiek, S., Vuister, G. W., Zhu, G., Pfeifer, J., and Bax, A. (1995) NMRPipe: A multidimensional spectral processing system based on UNIX pipes. *J. Biomol. NMR* 6, 277–293.
- (41) Keller, R. (2007) *The computer-aided resonance assignment tutorial*, Cantina-Verlag, Goldau, Switzerland.
- (42) Ahmed, M. A. M., Bamm, V. V., Harauz, G., and Ladizhansky, V. (2007) The BG21 isoform of Golli myelin basic protein is intrinsically disordered with a highly flexible amino-terminal domain. *Biochemistry* 46, 9700–9712.
- (43) Wang, Y., and Jardetzky, O. (2002) Probability-based protein secondary structure identification using combined NMR chemical-shift data. *Protein Sci.* 11, 852–861.
- (44) Shen, Y., Lange, O., Delaglio, F., Rossi, P., Aramini, J. M., Liu, G., Eletsky, A., Wu, Y., Singaraju, K. K., Lemak, A., Ignatchenko, A., Arrowsmith, C. H., Szyperski, T., Montelione, G. T., Baker, D., and Bax, A. (2008) Consistent blind protein structure generation from NMR chemical shift data. *Proc. Natl. Acad. Sci. U.S.A.* 105, 4685–4690.
- (45) Schwieters, C. D., Kuszewski, J. J., Tjandra, N., and Clore, G. M. (2003) The Xplor-NIH NMR molecular structure determination package. *J. Magn. Reson.* 160, 65–73.
- (46) Schwieters, C. D., Kuszewski, J. J., and Clore, G. M. (2006) Using Xplor-NIH for NMR molecular structure determination. *Prog. Nucl. Magn. Reson. Spectrosc.* 48, 47–62.
- (47) Nygaard, E., Mendz, G. L., Moore, W. J., and Martenson, R. E. (1984) NMR of a peptic peptide spanning the triprolyl sequence in myelin basic protein. *Biochemistry* 23, 4003–4010.
- (48) Fraser, P. E., and Deber, C. M. (1985) Structure and function of the proline-rich region of myelin basic protein. *Biochemistry* 24, 4593–4598.
- (49) Bennett, W. F., and Tieleman, D. P. (2009) *Free energies of lipid-lipid interactions in membranes*, Elsevier/ACS, Amsterdam.

- (50) Gao, X., and Wong, T. C. (2001) Molecular dynamics simulation of adrenocorticotropin (1–10) peptide in a solvated dodecylphosphocholine micelle. *Biopolymers* 58, 643–659.
- (51) Hess, B., Kutzner, C., Van Der Spoel, D., and Lindahl, E. (2008) GROMACS 4: Algorithms for highly efficient, load-balanced, and scalable molecular simulation. *J. Chem. Theory Comput.* 4, 435–447.
- (52) Humphrey, W., Dalke, A., and Schulten, K. (1996) VMD: Visual molecular dynamics. *J. Mol. Graphics* 14, 33–38.
- (53) Maxwell, K. L., and Davidson, A. R. (1998) Mutagenesis of a buried polar interaction in an SH3 domain: Sequence conservation provides the best prediction of stability effects. *Biochemistry* 37, 16172–16182.
- (54) Sibille, N., Huvent, I., Fauquant, C., Verdegem, D., Amniai, L., Leroy, A., Wieruszewski, J. M., Lippens, G., and Landrieu, I. (2012) Structural characterization by nuclear magnetic resonance of the impact of phosphorylation in the proline-rich region of the disordered Tau protein. *Proteins* 80, 454–462.
- (55) Kim, S. Y., Jung, Y., Hwang, G. S., Han, H., and Cho, M. (2011) Phosphorylation alters backbone conformational preferences of serine and threonine peptides. *Proteins* 79, 3155–3165.
- (56) Bamm, V. V., Ahmed, M. A., and Harauz, G. (2010) Interaction of myelin basic protein with actin in the presence of dodecylphosphocholine micelles. *Biochemistry* 49, 6903–6915.
- (57) Camilloni, C., De, S. A., Vranken, W. F., and Vendruscolo, M. (2012) Determination of secondary structure populations in disordered states of proteins using nuclear magnetic resonance chemical shifts. *Biochemistry* 51, 2224–2231.
- (58) Homchaudhuri, L., De Avila, M., Nilsson, S. B., Bessonov, K., Smith, G. S., Bamm, V. V., Musse, A. A., Harauz, G., and Boggs, J. M. (2010) Secondary structure and solvent accessibility of a calmodulin-binding C-terminal segment of membrane-associated myelin basic protein. *Biochemistry* 49, 8955–8966.
- (59) Kattnig, D. R., Bund, T., Boggs, J. M., Harauz, G., and Hinderberger, D. (2012) Lateral self-assembly of 18.5-kDa myelin basic protein (MBP) charge component-C1 on membranes. *Biochim. Biophys. Acta* 1818, 2636–2647.
- (60) Bailey, R. W., Dunker, A. K., Brown, C. J., Garner, E. C., and Griswold, M. D. (2001) Clusterin, a binding protein with a molten globule-like region. *Biochemistry* 40, 11828–11840.
- (61) Marsh, J. A., and Forman-Kay, J. D. (2010) Sequence determinants of compaction in intrinsically disordered proteins. *Biophys. J.* 98, 2383–2390.
- (62) Marsh, J. A., and Forman-Kay, J. D. (2012) Ensemble modeling of protein disordered states: Experimental restraint contributions and validation. *Proteins* 80, 556–572.
- (63) Bond, P. J., and Sansom, M. S. (2003) Membrane protein dynamics versus environment: Simulations of OmpA in a micelle and in a bilayer. *J. Mol. Biol.* 329, 1035–1053.
- (64) Musse, A. A., and Harauz, G. (2007) Molecular “negativity” may underlie multiple sclerosis: Role of the myelin basic protein family in the pathogenesis of MS. *Int. Rev. Neurobiol.* 79, 149–172.
- (65) Cross, T. A., Sharma, M., Yi, M., and Zhou, H. X. (2011) Influence of solubilizing environments on membrane protein structures. *Trends Biochem. Sci.* 36, 117–125.
- (66) Hornemann, S., von, S. C., Damberger, F. F., and Wüthrich, K. (2009) Prion protein-detergent micelle interactions studied by NMR in solution. *J. Biol. Chem.* 284, 22713–22721.
- (67) Galdiero, S., Russo, L., Falanga, A., Cantisani, M., Vitiello, M., Fattorusso, R., Malgieri, G., Galdiero, M., and Isernia, C. (2012) Structure and orientation of the gH625–644 membrane interacting region of herpes simplex virus type 1 in a membrane mimetic system. *Biochemistry* 51, 3121–3128.
- (68) Singarapu, K. K., Tonelli, M., Chow, D. C., Frederick, R. O., Westler, W. M., and Markley, J. L. (2011) Structural characterization of Hsp12, the heat shock protein from *Saccharomyces cerevisiae*, in aqueous solution where it is intrinsically disordered and in detergent micelles where it is locally α -helical. *J. Biol. Chem.* 286, 43447–43453.
- (69) Tulumello, D. V., and Deber, C. M. (2012) Efficiency of detergents at maintaining membrane protein structures in their biologically relevant forms. *Biochim. Biophys. Acta* 1818, 1351–1358.
- (70) Harauz, G., and Ladizhansky, V. (2008) Structure and dynamics of the myelin basic protein family by solution and solid-state NMR. In *Myelin Basic Protein* (Boggs, J. M., Ed.) pp 197–232, Nova Science Publishers, New York.

Supporting Information

Solution NMR structure and molecular dynamics simulations of 18.5-kDa myelin basic protein segment (S72-S107) in association with dodecylphosphocholine micelles

Mumdooh A.M Ahmed¹⁻³,
Miguel De Avila¹,
Eugenia Polverini⁴,
Kyrylo Bessonov¹,
Vladimir V. Bamm¹,
George Harauz^{1*}.

Departments of ¹Molecular and Cellular Biology, and ²Physics,
University of Guelph, 50 Stone Road East, Guelph, Ontario, N1G 2W1, Canada;

³Department of Physics, Faculty of Science at Suez, Suez-Canal University, Suez, Egypt;

⁴Department of Physics, University of Parma, V. le Usberti, 7/A - Campus, 43124 Parma, Italy.

Supporting Figure S1 – Plot showing re-scored CS-ROSETTA all atom energy compared to the RMSD of the C_α chemical shifts relative to the lowest energy structure. The 1,000 models produced by CS-ROSETTA are shown in this plot. Convergence towards the lowest energy structure suggests a successful structural prediction.

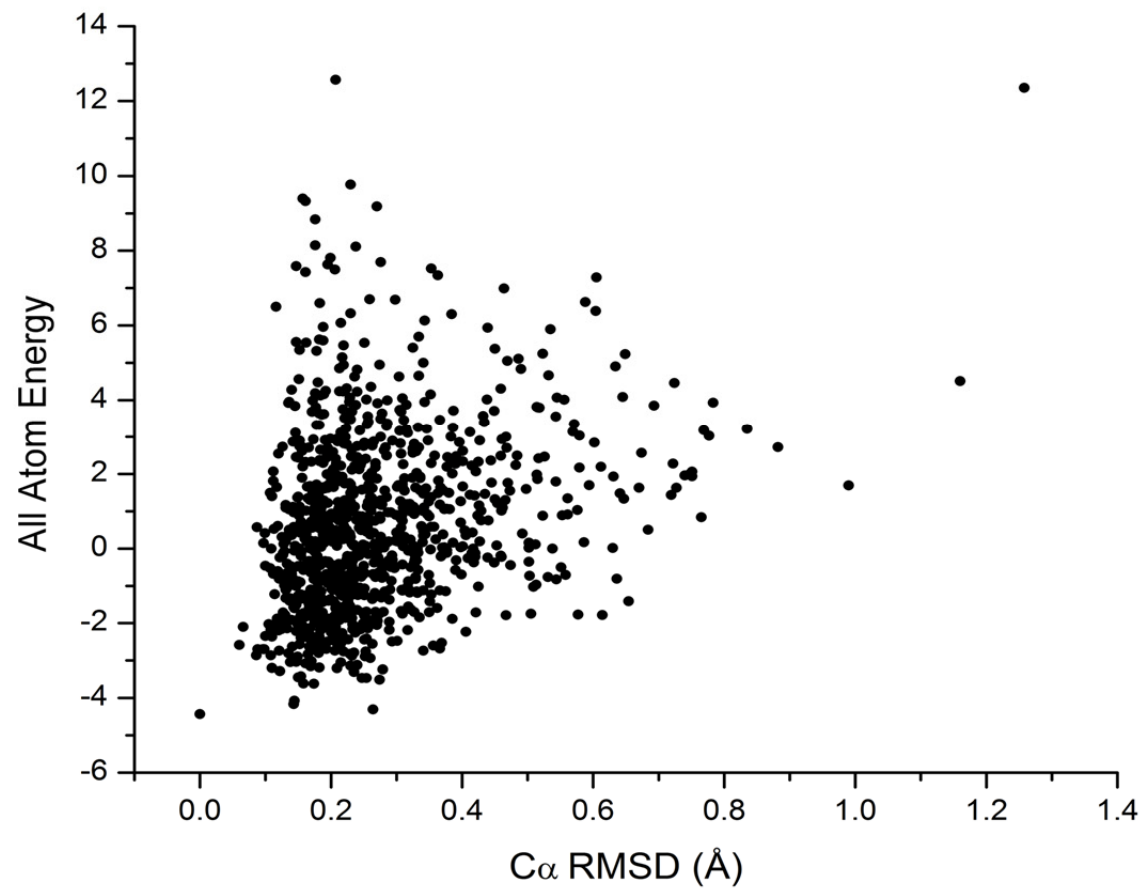


Figure S2 – Strip plots extracted from the HN(CA)CO spectrum (top), and the HNCACB spectrum (bottom), used for backbone assignments of the residues of the α 2-peptide in equimolar association with the Fyn-SH3-somain. The strip plots show the connectivity between the S28 and S36 residues of the α 2-peptide.

^{15}N (ppm)

115.33 122.07 109.71 120.55 109.86 120.80 110.05 121.77 121.46

170
172
174
176
178
180
182
184
 ^{13}C (ppm)

S28 Q29 G30 K31 G32 R33 G34 L35 S36

12
18
24
30
36
42
48
54
60
66
72 ^1H (ppm)

Table S1 – The ^1H and ^{13}C chemical shifts of the $\alpha 2$ -peptide of 18.5-kDa myelin basic protein, referenced to DSS (2,2-dimethylsilapentane-5-sulphonic acid). These data have been deposited in the BioMagResBank (www.bmrb.wisc.edu) with accession number 18520.

#	AA	N	CO	CA	CB	CG G1	CG2	CD D1	CD2	CE	H	HA A2	HB B2	HB3	HG G1 G12	HG13	HG2	HG3	HD1	HD2	HD3	HE2	HE3	
1	SER	115.900	--	58.110	63.310	--	--	--	--	--	8.281	4.210	3.721	--	--	--	--	--	--	--	--	--	--	
2	GLN	122.100	175.731	55.720	29.220	33.320	--	--	--	--	8.342	4.122	1.782	1.742	--	--	2.120	--	--	--	--	--	--	--
3	HIS	120.300	175.541	55.730	29.830	--	--	--	--	--	8.443	4.493	3.033	2.923	--	--	--	--	--	--	--	--	--	--
4	GLY	110.300	174.051	45.400	--	--			--	--	8.374	3.764	--	--	--	--	--	--	--	--	--	--	--	--
5	ARG	120.800	176.861	55.850	30.550	26.750		43.500	--	--	8.245	4.245	1.695	1.575	--	--	1.445	--	--	3.000	--	--	--	--
6	THR	116.100	174.771	61.960	69.560	--	21.560	--	--	--	8.246	4.126	4.036	--	4.336	--	1.016	--	--	--	--	--	--	--
7	GLN	122.000	175.581	55.870	29.370	33.470	--	--	--	--	8.397	4.127	1.837	1.797	--	--	2.147	--	--	--	--	--	--	--
8	ASP	121.400	175.891	54.380	40.880	--	--	--	--	--	8.188	4.388	2.488	2.388	--	--	--	--	--	--	--	--	--	--
9	GLU	120.600	175.901	55.690	30.890	36.190	--	--	--	--	8.059	4.149	1.819	1.749	--	--	2.190	2.079	--	--	--	--	--	--
10	ASN	124.100	174.521	51.910	39.410	--	--	--	--	--	8.951	4.681	2.851	2.561	--	--	--	--	--	--	--	--	--	--
11	PRO	136.800	--	65.110	32.411	27.611	--	51.110	--	--	--	4.251	2.321	--	--	--	2.011	--	--	3.821	3.611	--	--	--
12	VAL	119.100	177.423	66.312	31.112	22.712	21.812	--	--	--	8.191	3.612	2.171	--	0.891	--	0.911	--	--	--	--	--	--	--
13	VAL	120.000	177.524	66.813	31.513	22.613	21.213	--	--	--	7.431	3.471	2.121	--	0.931	--	0.861	--	--	--	--	--	--	--
14	HIS	116.900	176.525	59.714	29.314	--	--	--	--	--	8.321	3.921	3.081	2.991	--	--	--	--	--	--	--	--	--	--
15	PHE	118.600	177.326	61.215	39.150	--	--	--	--	--	7.772	3.972	3.092	3.022	--	--	--	--	--	--	--	--	--	--
16	PHE	116.500	177.627	61.716	39.216	--	--	--	--	--	7.892	3.922	2.962	2.882	--	--	--	--	--	--	--	--	--	--
17	LYS	117.900	178.028	59.717	32.317	25.917	--	29.417	--	41.617	8.432	3.717	1.622	--	--	--	1.162	--	--	1.492	--	2.742	2.642	--
18	ASN	115.200	176.029	54.518	38.518	--	--	--	--	--	7.462	4.272	2.472	2.342	--	--	--	--	--	--	--	--	--	--
19	ILE	117.600	175.930	62.919	37.819	27.919	17.519	13.219	--	--	7.172	3.682	1.612	--	1.192	0.832	0.622	--	0.432	--	--	--	--	--
20	VAL	113.300	175.531	62.220	32.200	21.520	20.320	--	--	--	7.212	3.942	2.012	--	0.722	--	0.722	--	--	--	--	--	--	--
21	THR	117.300	182.232	58.221	69.521	--	20.821	--	--	--	7.621	4.322	3.952	--	--	--	0.952	--	--	--	--	--	--	--
22	PRO	138.600	176.933	62.822	31.722	27.220	--	50.522	--	--	--	4.242	2.122	--	--	--	1.792	--	--	3.712	3.532	--	--	--
23	ARG	121.500	176.334	55.823	30.623	26.923	--	42.723	--	--	8.442	4.162	1.692	1.572	--	--	--	1.452	--	--	3.000	--	--	--

24	THR	118.500	182.335	59.724	69.624	--	21.124	--	--	--	8.152	4.362	3.912	--	--	--	1.052	--	--	--	--	--	
25	PRO	140.500	--	61.225	30.525	27.250	--	50.825	--	--	--	4.493	1.693	--	--	--	1.843	--	--	3.725	3.525	--	--
26	PRO	136.700	--	61.126	30.526	27.126	--	50.126	--	--	--	4.523	1.713	--	--	--	1.853	--	--	3.633	3.433	--	--
27	PRO	135.300	177.381	62.827	31.727	27.227	--	50.327	--	--	--	4.253	1.733	--	--	--	1.843	--	--	3.633	3.463	--	--
28	SER	115.800	174.739	58.128	63.428	--	--	--	--	--	8.328	4.213	3.663	3.728	--	--	--	--	--	--	--	--	--
29	GLN	122.000	176.340	55.729	29.129	33.529	--	--	--	--	8.363	4.183	1.963	1.929	--	--	2.193	--	--	--	--	--	--
30	GLY	109.900	174.411	45.300	--	--	--	--	--	--	8.313	--	--	--	--	--	--	--	--	--	--	--	--
31	LYS	120.800	177.242	56.131	32.731	24.431	--	28.731	--	41.831	8.183	4.143	1.673	1.573	--	--	1.263	1.223	--	1.483		2.793	--
32	GLY	109.900	174.043	45.320	--	--	--	--	--	--	8.393	--	--	--	--	--	--	--	--	--	--	--	--
33	ARG	120.600	176.944	55.933	30.333	26.733	--	42.933	--	--	8.193	4.143	1.693	1.573	--	--	1.443	--	--	3.013	--	--	--
34	GLY	110.000	174.045	45.340	--	--	--	--	--	--	8.434	--	--	--	--	--	--	--	--	--	--	--	--
35	LEU	121.800	176.746	54.835	42.235	26.735	--	24.735	22.835	--	8.054	4.234	1.454	--	1.434	--	--	--	0.734	0.684		--	--
36	SER	121.300	178.547	59.736	64.636	--	--	--	--	--	7.784	4.074	3.654	--	--	--	--	--	--	--	--	--	--